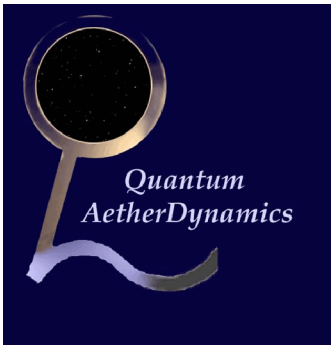

Quantum AetherDynamics Institute (QADI)

V_{ud} and First-Row CKM Unitarity as a QMU Ledger Closure

David W. Thomson III
Quantum AetherDynamics Institute (QADI), Alma, Illinois, USA
ORCID: 0000-0002-5830-5427

Version 1.0 – February 17, 2026

This article is published by the Quantum AetherDynamics Institute (QADI).

It develops the Aether Physics Model (APM)

Abstract

We extend the Aether Physics Model (APM) weak-sector program to the first-row unitarity relation $|V_{ud}|^2 + |V_{us}|^2 + |V_{ub}|^2 = 1$ by reframing it as a QMU ledger-closure identity in a quark packing basis. The extraction of V_{ud} from superallowed nuclear beta decays is rewritten in a strictly QMU narrative: the observed constancy of corrected $\mathcal{F}t$ values is treated as a statement of vector-current closure under an Aether holonomy map, while standard "radiative" and "nuclear-structure" corrections are reorganized into (i) holonomy boundary terms and (ii) charge-basis conversion terms governed by the APM unified charge equation and implemented operationally by the Charge Conversion Factor (CCF) when bridging to SI. All primary inputs are dimensionless or reducible to QMU invariants; SI appears only in an appendix used to translate standard experimental reporting conventions.

Keywords: Aether Physics Model; Quantum Measurement Units; superallowed beta decay; V_{ud}; Cabibbo angle; CKM unitarity; holonomy; basis closure

1 Introduction

Institutional attribution follows the QADI reference identity Thomson III [2025].

In mainstream notation, the first-row CKM unitarity test is written

$$|V_{ud}|^2 + |V_{us}|^2 + |V_{ub}|^2 = 1. \tag{1}$$

Within the APM/QMU framework, (1) is treated as a *basis-closure statement* rather than an axiom of a matrix model: quark-sector "mixing parameters" are overlap invariants of packing states induced by 5D-to-4D holonomy, and the squared moduli represent completeness weights in the holonomy-induced inner product. Historically, the same first-row structure is anchored by the Cabibbo and CKM constructions in standard notation Cabibbo [1963], Kobayashi and Maskawa [1973], Wolfenstein [1983].

The purpose of this paper is threefold. First, define V_{ud} in QMU-native language as a packing overlap invariant. Second, map the superallowed $\mathcal{F}t$ constancy program into a ledger-first closure form. Third, express first-row unitarity as a closure residual that separates (A) genuine holonomy leakage from (B) charge-basis conversion and normalization drift that violates the APM charge-basis bookkeeping Thomson [2025a].

Why this matters now. The Particle Data Group (PDG) review emphasizes that first-row unitarity shows a persistent $\sim 2\sigma$ tension with unity when superallowed V_{ud} is combined with kaon-sector V_{us} averages; the tension can be interpreted as unaccounted uncertainties (radiative, nuclear-structure, or lattice inputs) or new physics in standard language Particle Data Group [2024]. In the QMU ledger, the same empirical fact is re-expressed as a closure check on an Aether-induced basis map.

2 Ledger anchor and charge-basis discipline

A canonical electromagnetic closure is

$$A_u \,\mathrm{curl} = {F_q}^2 \, {\lambda_C}^2, \tag{2}$$

used here only as a template for what "ledger closure" means: a propagation/normalization constant is decomposed into QMU primitives without mixed nomenclature.

Charge-basis discipline (unified charge equation and CCF). In QMU, charge is square-charge. The APM distinguishes singular and distributed square-charge bases and relates them by the *unified charge equation*

$$e^2 = 8\pi\,\alpha\,{e_{\mathrm{emax}}}^2, \tag{3}$$

with α the fine-structure constant and ${e_{\mathrm{emax}}}^2$ the distributed square-charge in the APM basis Thomson [2025a]. For SI reporting and SI↔QMU translation, the operational bridge is the *Charge Conversion Factor (CCF)*

$$\mathrm{CCF} := \frac{{e_{\mathrm{emax}}}^2}{e}, \tag{4}$$

where e is the SI elementary charge magnitude. The CCF is the conversion factor used to translate SI charge-based units to QMU and back, while (3) enforces the APM charge-basis relationship internally.

3 Data-facing closure target

This section records the numerical closure target that the APM/QMU derivation must reproduce.

3.1 Superallowed $0^+ \to 0^+$ input for V_{ud}

The PDG review summarizes the Hardy–Towner superallowed program and reports the superallowed result

$$V_{ud} = 0.97367(32) \qquad \text{(superallowed, total uncertainty)}, \tag{5}$$

including an explicit nuclear-structure uncertainty budget and modern treatments of the "inner" correction via γW box analyses Particle Data Group [2024], Hardy and Towner [2020], Czarnecki et al. [2019], Seng et al. [2019], Marciano and Sirlin [1986].

3.2 Kaon-sector V_{us} and negligible V_{ub}

For the first-row test, the PDG review adopts a kaon-sector average that includes a scale factor reflecting internal tensions between $K_{\ell 3}$ and $K_{\mu 2}$ determinations:

$$V_{us} = 0.22431(85) \qquad \text{(kaon-sector average with scale factor)}. \tag{6}$$

The contribution $|V_{ub}|^2$ is negligible at the level of the row-1 closure test and is typically dropped in the discussion Particle Data Group [2024].

3.3 First-row residual

The PDG review reports the combined first-row consistency check

$$|V_{ud}|^2 + |V_{us}|^2 + |V_{ub}|^2 = 0.9983(6)(4), \tag{7}$$

corresponding to an overall $\sim 2\sigma$ deviation from unity Particle Data Group [2024]. In this paper, (7) is the empirical closure target that the QMU ledger derivation must explain.

4 QMU reframing of V_{ud}

4.1 Overlap-invariant definition

We define the up–down mixing parameter as a dimensionless overlap invariant of packing states:

$$V_{ud} := \langle u \,|\, d \rangle_{\mathcal{H}}, \tag{8}$$

where $\mathcal{H}$ is the holonomy-induced inner product determined by the 5D-to-4D projection map. The squared modulus $|V_{ud}|^2$ is then a completeness weight; the unitarity condition (1) becomes a basis-closure identity in $\mathcal{H}$.

4.2 Holonomy defect parametrization

Introduce a closed-path defect one-form $\delta\omega_{ud}$ governing the $u \to d$ overlap channel, and define the dimensionless defect amplitude

$$\varepsilon_{ud} := \frac{1}{2\pi} \oint_{\gamma_{ud}} \delta\omega_{ud}, \tag{9}$$

with $\varepsilon_{ud} = 0$ corresponding to exact overlap conservation in that channel. A minimal closure-consistent expansion is

$$|V_{ud}|^2 = 1 - \varepsilon_{ud}^2 + O(\varepsilon_{ud}^3), \tag{10}$$

so that deviations from unity are directly tied to a holonomy leakage parameter rather than an abstract matrix element.

Interpretation. The choice (10) is bookkeeping: the *squared* overlap is the natural closure weight, and the leading closure defect is quadratic in a small dimensionless leakage amplitude.

5 Superallowed $\mathcal{F}t$ constancy as a QMU closure statement

5.1 What the data say

The superallowed $0^+ \to 0^+$ nuclear beta decays provide a high-precision determination of V_{ud} by establishing the constancy of corrected $\mathcal{F}t$ values across many nuclei Hardy and Towner [2020], Particle Data Group [2024]. In standard language, this is CVC plus calculable correction factors.

5.2 QMU master architecture

Define a QMU-normalized corrected lifetime invariant

$$\mathcal{T}_V := F_q \, \mathcal{F}t, \tag{11}$$

which is dimensionless because F_q is a frequency scale and $\mathcal{F}t$ carries time dimension. The CVC constancy statement becomes

$$\mathcal{T}_V^{(i)} = \mathcal{T}_V^{(*)} \quad \text{for all superallowed transitions } i, \tag{12}$$

up to calculable boundary and basis-conversion terms.

We write the QMU extraction formula as

$$|V_{ud}|^2 = \frac{\mathcal{K}_V}{\mathcal{T}_V^{(*)}} \frac{1}{\mathcal{B}_V}, \tag{13}$$

where: (i) $\mathcal{K}_V$ is a universal QMU constant (the weak-sector analogue of an electromagnetic closure constant), (ii) $\mathcal{B}_V$ is a dimensionless boundary factor collecting holonomy boundary terms and APM charge-basis conversion terms.

5.3 Radiative corrections as boundary terms

The PDG review emphasizes modern treatments of the "inner" correction (including γW box analyses) and its impact on the extracted V_{ud} Particle Data Group [2024], Czarnecki et al. [2019], Seng et al. [2019], Marciano and Sirlin [1986]. In the QMU narrative, such terms are organized as holonomy boundary contributions:

$$\mathcal{B}_V = \mathcal{B}_{\text{hol}}\, \mathcal{B}_{\text{map}}, \tag{14}$$

with $\mathcal{B}_{\text{hol}}$ a pure holonomy boundary factor and $\mathcal{B}_{\text{map}}$ a charge-basis conversion factor constrained by the unified charge equation (3) and implemented by the CCF when translating to/from SI Thomson [2025a]. The operational benefit of (14) is that a persistent first-row residual can be traced to either geometry (holonomy leakage) or bookkeeping (charge-basis conversion inconsistency), but not both simultaneously.

6 Milestone M1: Weak-sector universal constant $\mathcal{K}_V$ from a normalized holonomy connection

This milestone supplies the first concrete object needed to make the program parameter-free: an explicit *vector-channel* holonomy connection whose (i) closed-cycle closure and (ii) forward-time restriction generate the universal constant $\mathcal{K}_V$ and the holonomy boundary factor $\mathcal{B}_{\text{hol}}$ appearing in (13) and (14).

6.1 Action-normalized weak connection one-form

In the QMU ledger, a natural way to produce a dimensionless holonomy is to normalize an action increment by a QMU action scale. We reuse the electron action scale

$$h_e := m_{\text{e}}\, {\lambda_C}^2\, F_q, \tag{15}$$

not because the weak sector is "electromagnetic," but because h_e is a ledger-stable QMU action quantum associated with the Aether-unit chronovibration bookkeeping.

Let $S_{5,V}$ be the 5D vector-channel packing action functional for the $u \leftrightarrow d$ channel along the full 5D chronovibrational cycle Γ. Define the 5D vector connection one-form by

$$\omega_{5,V} := \frac{dS_{5,V}}{h_e}. \tag{16}$$

Let Π denote the 5D→4D projection induced by the forward-time observational restriction. Define the 4D projected action $S_{4,V} := \Pi S_{5,V}$ and the induced 4D connection

$$\omega_{4,V} := \frac{dS_{4,V}}{h_e}. \tag{17}$$

The defect one-form is then

$$\delta\omega_V := \omega_{5,V} - \omega_{4,V}. \tag{18}$$

By construction, $\omega_{5,V}$, $\omega_{4,V}$, and $\delta\omega_V$ are dimensionless one-forms in the QMU ledger.

M1 toy model (loxodrome winding + minimal twist). As an existence proof that the obstruction bookkeeping can generate concrete numbers, introduce a schematic connection split:

$$\omega_{5,V} = \omega_V^{(0)} + \omega_V^{(\mathrm{tw})}, \qquad \omega_{4,V} = \Pi\omega_V^{(0)} + \Pi\omega_V^{(\mathrm{tw})}. \tag{19}$$

Assume the baseline loxodrome sector yields a pure winding number $n_V \in \mathbb{Z}$, while the twist sector contributes a small seam-normalization term η_V sensitive to packing:

$$\frac{1}{2\pi}\oint_{\gamma_+}(I-\Pi)\omega_V^{(0)} = n_V, \qquad \frac{1}{2\pi}\oint_{\gamma_+}(I-\Pi)\omega_V^{(\mathrm{tw})} = \eta_V, \qquad |\eta_V| \ll 1. \tag{20}$$

This yields a minimal explicit form $\Delta_V = n_V + \eta_V$, which is then reduced to the domain-seam description in M3–M5 by writing n_V as the integer seam class and η_V as the small correction that the seam-lock normalization must explain.

6.2 5D closure integer and forward-time restriction

Define the full-cycle 5D holonomy and its integer closure index by

$$\Theta_V^{(5)} := \frac{1}{2\pi}\oint_{\Gamma}\omega_{5,V}, \qquad \Theta_V^{(5)} = n_V \in \mathbb{Z}. \tag{21}$$

Let $\gamma_+ \subset \Gamma$ denote the forward-time (4D-visible) leg. Define the forward-time 5D phase advance

$$\Theta_V^{(+)} := \frac{1}{2\pi}\oint_{\gamma_+}\omega_{5,V}, \tag{22}$$

and the forward-time defect amplitude

$$\Delta_V := \frac{1}{2\pi}\oint_{\gamma_+}\delta\omega_V. \tag{23}$$

The point of the APM holonomy picture is that 5D closure (21) does *not* force the restricted forward-time defect Δ_V to vanish.

Introduce a sampling fraction

$$\eta_V := \frac{\Theta_V^{(+)}}{\Theta_V^{(5)}} = \frac{1}{n_V}\Theta_V^{(+)}, \qquad 0 < \eta_V < 1, \tag{24}$$

so η_V measures how much of the full-cycle vector rotation is sampled on the forward-time leg.

6.3 From holonomy to the universal constant $\mathcal{K}_V$

Define the forward-leg vector turn count

$$N_V^{(+)} := \Theta_V^{(+)} = \eta_V \, n_V. \tag{25}$$

A QMU-native normalization choice that makes $\mathcal{K}_V$ dimensionless and geometry-tied is

$$\mathcal{K}_V := \frac{1}{N_V^{(+)}} = \frac{1}{\eta_V \, n_V}. \tag{26}$$

With (26), the master extraction becomes

$$|V_{ud}|^2 = \frac{1}{\eta_V \, n_V} \, \frac{1}{\mathcal{T}_V^{(*)}} \, \frac{1}{\mathcal{B}_V}, \qquad \mathcal{B}_V = \mathcal{B}_{\rm hol}\mathcal{B}_{\rm map}. \tag{27}$$

6.4 Holonomy boundary factor $\mathcal{B}_{\rm hol}$

Define the holonomy boundary factor as the real, dimensionless multiplier converting idealized forward turns into effective observable turns:

$$N_{V,\rm eff}^{(+)} := N_V^{(+)} \, \mathcal{B}_{\rm hol}^{-1}, \qquad \mathcal{B}_{\rm hol} := \frac{N_V^{(+)}}{N_{V,\rm eff}^{(+)}}. \tag{28}$$

A defect-controlled parametrization is

$$\mathcal{B}_{\rm hol}^{-1} = 1 - \varepsilon_V^2 + O(\varepsilon_V^3), \qquad \varepsilon_V := \Delta_V + \varepsilon_{V,\rm stitch}, \tag{29}$$

where $\varepsilon_{V,\rm stitch}$ is the discrete stitching contribution fixed by the seam taxonomy (M3–M4).

6.5 Deliverable for M1

Milestone M1 is complete once an explicit Aether-packing action $S_{5,V}$ is specified for the vector channel, so that $\omega_{5,V}$ and $\omega_{4,V}$ are explicit and the following quantities can be evaluated:

$$n_V = \frac{1}{2\pi} \oint_\Gamma \omega_{5,V} \in \mathbb{Z}, \qquad \eta_V = \frac{1}{n_V} \frac{1}{2\pi} \oint_{\gamma_+} \omega_{5,V}, \qquad \Delta_V = \frac{1}{2\pi} \oint_{\gamma_+} (\omega_{5,V} - \omega_{4,V}). \tag{30}$$

In M2 we enforce the chronovibration restriction explicitly by parameterizing γ_+ on the Aether unit and showing that Δ_V need not vanish even when $n_V \in \mathbb{Z}$.

7 Milestone M2: Chronovibration restriction via a torsion-density action

Milestone M2 implements the forward-time restriction γ_+ explicitly and shows, in a torsion-density model, how a nonzero forward-time holonomy defect survives even when the full 5D cycle closes with an integer index n_V.

7.1 Torsion density as the vector-channel action primitive

Let $\mathcal{M}_5$ denote the 5D Aether-packing manifold. Let $\mathcal{T}_V$ denote a vector-channel torsion 3-form built from the relevant Aether-unit connection and packing frames. Let $\Sigma(\Gamma) \subset \mathcal{M}_5$ be a ribbon (a 3D swept surface) associated with the full cycle Γ, and let $\Sigma(\gamma_+) \subset \Sigma(\Gamma)$ denote the forward-time ribbon. Define

$$S_{5,V}(\Gamma) := \int_{\Sigma(\Gamma)} \mathcal{T}_V, \qquad S_{5,V}(\gamma_+) := \int_{\Sigma(\gamma_+)} \mathcal{T}_V, \tag{31}$$

and

$$\omega_{5,V} := \frac{dS_{5,V}}{h_e}. \tag{32}$$

7.2 5D closure index

Ledger closure requires integer holonomy:

$$\Theta_V^{(5)} := \frac{1}{2\pi} \oint_\Gamma \omega_{5,V} = \frac{1}{2\pi\, h_e} \int_{\Sigma(\Gamma)} \mathcal{T}_V = n_V \in \mathbb{Z}. \tag{33}$$

7.3 Forward-time sampling fraction η_V

$$\Theta_V^{(+)} := \frac{1}{2\pi} \oint_{\gamma_+} \omega_{5,V} = \frac{1}{2\pi\, h_e} \int_{\Sigma(\gamma_+)} \mathcal{T}_V, \tag{34}$$

and

$$\eta_V := \frac{\Theta_V^{(+)}}{\Theta_V^{(5)}} = \frac{\displaystyle\int_{\Sigma(\gamma_+)} \mathcal{T}_V}{\displaystyle\int_{\Sigma(\Gamma)} \mathcal{T}_V}. \tag{35}$$

7.4 4D projection and the defect Δ_V

Define the 4D-projected action by replacing $\mathcal{T}_V$ with $\Pi\mathcal{T}_V$ on $\Sigma(\gamma_+)$:

$$S_{4,V}(\gamma_+) := \int_{\Sigma(\gamma_+)} \Pi\mathcal{T}_V, \qquad \omega_{4,V} := \frac{dS_{4,V}}{h_e}. \tag{36}$$

Then

$$\begin{aligned} \Delta_V &:= \frac{1}{2\pi} \oint_{\gamma_+} (\omega_{5,V} - \omega_{4,V}) \\ &= \frac{1}{2\pi\, h_e} \int_{\Sigma(\gamma_+)} (\mathcal{T}_V - \Pi\mathcal{T}_V) = \frac{1}{2\pi\, h_e} \int_{\Sigma(\gamma_+)} (I - \Pi)\mathcal{T}_V. \end{aligned} \tag{37}$$

7.5 Deliverable for M2

Milestone M2 is complete once $\mathcal{T}_V$ is specified in terms of Aether-unit geometry so that:

$$n_V = \frac{1}{2\pi h_e} \int_{\Sigma(\Gamma)} \mathcal{T}_V \in \mathbb{Z}, \qquad \eta_V = \frac{\int_{\Sigma(\gamma_+)} \mathcal{T}_V}{\int_{\Sigma(\Gamma)} \mathcal{T}_V}, \qquad \Delta_V = \frac{1}{2\pi h_e} \int_{\Sigma(\gamma_+)} (I - \Pi)\mathcal{T}_V. \tag{38}$$

8 Milestone M3: Domain taxonomy and seam torsion quantization

Milestone M3 fixes a minimal, explicit domain decomposition and reduces Δ_V to seam (stitching) data classified by a discrete obstruction index.

8.1 Minimal antipodally paired domain decomposition

$$\Sigma(\gamma_+) = \bigcup_{i=1}^{8} \Sigma_i, \qquad \Sigma_i \cap \Sigma_j = \emptyset \quad (i \neq j), \tag{39}$$

with antipodal pairing $i \leftrightarrow \bar{i}$. Let seams be $\mathcal{E}_{ij} := \partial\Sigma_i \cap \partial\Sigma_j$ and $\mathcal{E} = \{\mathcal{E}_{ij}\}$.

8.2 Bulk–seam decomposition

On each Σ_i,

$$\mathcal{T}_V|_{\Sigma_i} = d\mathcal{Q}_i \; + \; \mathcal{T}_{V,\mathrm{seam}}|_{\Sigma_i}. \tag{40}$$

Using (37),

$$\begin{aligned} \Delta_V &= \frac{1}{2\pi h_e} \sum_{i=1}^{8} \int_{\Sigma_i} (I - \Pi)\mathcal{T}_V \\ &= \frac{1}{2\pi h_e} \sum_{i=1}^{8} \left(\int_{\partial\Sigma_i} (I - \Pi)\mathcal{Q}_i + \int_{\Sigma_i} (I - \Pi)\mathcal{T}_{V,\mathrm{seam}} \right). \end{aligned} \tag{41}$$

8.3 Antipodal cancellation of bulk

Impose

$$\int_{\partial\Sigma_{\bar{i}}} (I - \Pi)\mathcal{Q}_{\bar{i}} = -\int_{\partial\Sigma_i} (I - \Pi)\mathcal{Q}_i, \tag{42}$$

so

$$\sum_{i=1}^{8} \int_{\partial\Sigma_i} (I - \Pi)\mathcal{Q}_i = 0, \tag{43}$$

and Δ_V is controlled by seam torsion.

8.4 Seam torsion as a jump cocycle

Across seam $\mathcal{E}_{ij}$,

$$\Delta\mathcal{Q}_{ij} := \mathcal{Q}_j - \mathcal{Q}_i \quad \text{on } \mathcal{E}_{ij}. \tag{44}$$

Define the dimensionless seam phase jump

$$\delta\varphi_{ij} := \frac{1}{h_e} \int_{\mathcal{E}_{ij}} (I - \Pi)\Delta\mathcal{Q}_{ij}. \tag{45}$$

Then

$$\Delta_V = \frac{1}{2\pi} \sum_{\mathcal{E}_{ij} \in \mathcal{E}} \sigma_{ij}\, \delta\varphi_{ij}, \qquad \sigma_{ij} \in \{+1, -1\}. \tag{46}$$

8.5 Quantized seam increments and the obstruction index τ_V

Impose quantized seam increments in octant steps:

$$\delta\varphi_{ij} = m_{ij}\,\frac{\pi}{4}\,\Xi_V, \qquad m_{ij} \in \mathbb{Z}, \tag{47}$$

so

$$\Delta_V = \frac{\Xi_V}{8}\,\tau_V, \tag{48}$$

where

$$\tau_V := \sum_{\mathcal{E}_{ij}\in\mathcal{E}} \sigma_{ij}\, m_{ij} \in \mathbb{Z}. \tag{49}$$

8.6 M3 deliverable

Milestone M3 is complete once the seam graph and orientation conventions are fixed so that τ_V is well-defined and Δ_V reduces to the discrete spectrum (48).

9 Milestone M4: Wrap quantization and admissible obstruction classes

Milestone M4 restricts admissible obstruction indices by octant symmetry, antipodal pairing, and low-seam-energy assumptions.

9.1 Octant generator

$$\Delta\theta_{\text{oct}} := \frac{2\pi}{8} = \frac{\pi}{4}. \tag{50}$$

9.2 Wrap number and loop constraints

Let $\mathcal{L}_0$ be a primitive seam loop with edge-count $w_0 \in \mathbb{N}$. In the simplest octant loxodrome,

$$w_0 = 8. \tag{51}$$

9.3 Parity constraint

Antipodal pairing in the minimal CP-even octant model enforces

$$\tau_V \equiv 0 \pmod 2. \tag{52}$$

9.4 Admissible τ_V values in the low-seam sector

For $|m_{ij}| \le 1$ on a one-wrap loop, $|\tau_V| \le w_0$. With $w_0 = 8$ and (52),

$$\tau_V \in \{0, \pm 2, \pm 4, \pm 6, \pm 8\}. \tag{53}$$

9.5 Nuclear packing lift note (bridge for experimentalists)

The superallowed environment adds Coulomb and isospin-breaking structure that is treated in standard analyses as nucleus-dependent corrections Hardy and Towner [2020], Particle Data Group [2024]. In this program, those effects are identified with domain-boundary slips and seam-energy sector changes: they modify the prepared stitching class (hence $\{m_{ij}\}$, κ_V, and potentially the allowed sector) rather than introducing free continuous normalization drift. This is the intended bridge from "nuclear-structure corrections" to Aether packing geometry.

9.6 M4 deliverable

Milestone M4 is complete once $\mathcal{L}_0$ is specified for the $u \leftrightarrow d$ vector channel and the admissible set (53) is committed (or replaced by a stronger selection rule if required by the explicit packing symmetry).

10 Milestone M5: Charge-basis conversion, basis-map insertion, and toroidal seam-lock normalization

Milestone M5 inserts the APM charge-basis conversion discipline into the torsion bookkeeping and fixes the seam normalization Ξ_V as a *geometric* seam-lock multiplier (toroidal invariance) times a *basis-map* multiplier $\mathcal{M}_V(\alpha)$ fixed by the explicit packing map and constrained by the unified charge equation.

10.1 Unified charge equation and Charge Conversion Factor (CCF)

The APM unified charge equation is

$$e^2 = 8\pi\,\alpha\,{e_{\mathrm{emax}}}^2, \tag{54}$$

equivalently ${e_{\mathrm{emax}}}^2 = e^2/(8\pi\alpha)$ Thomson [2025a]. When bridging to SI reporting conventions, the operational conversion factor is the Charge Conversion Factor (CCF), defined by

$$\mathrm{CCF} := \frac{{e_{\mathrm{emax}}}^2}{e}, \tag{55}$$

and used to translate SI charge-based units to QMU and back, without altering the internal APM charge-basis identity (54).

10.2 Toroidal invariance principle for the forward-time projection

In the APM chronovibration picture, the 5D loxodrome projects into 4D as a tubular cardioid. For ledger purposes we treat this projection as a torus with major radius R (winding path scale) and minor radius r (tube thickness). We impose the *Toroidal Invariance Principle*:

$$R\,r = {\lambda_C}^2. \tag{56}$$

Because the torus area factorizes as $A = (2\pi R)(2\pi r) = 4\pi^2(Rr)$, (56) enforces a ledger-stable projection area $A = 4\pi^2 {\lambda_C}^2$ across species and channels. This is the geometric lock that prevents continuous normalization drift in the distributed square-charge basis.

10.3 Where the basis map enters the torsion action

Write the torsion density in factored form

$$\mathcal{T}_V = \mathcal{T}_{V,0}\, \mathcal{M}_V(\alpha), \tag{57}$$

where $\mathcal{T}_{V,0}$ is geometric and $\mathcal{M}_V(\alpha)$ is the channel basis-map multiplier fixed by the explicit packing map and constrained by the unified charge equation (54). Then

$$\Delta_V = \frac{1}{2\pi h_e} \int_{\Sigma(\gamma_+)} (I - \Pi)\mathcal{T}_V \approx \mathcal{M}_V(\alpha)\, \frac{1}{2\pi h_e} \int_{\Sigma(\gamma_+)} (I - \Pi)\mathcal{T}_{V,0}. \tag{58}$$

As in M3, write $\Delta_V = \frac{1}{8}\tau_V\, \Xi_V(\alpha)$; then the factorization implies

$$\Xi_V(\alpha) = \Xi_{V,0}\, \mathcal{S}_{\text{tor}}\, \mathcal{M}_V(\alpha), \tag{59}$$

where $\mathcal{S}_{\text{tor}}$ is the toroidal seam-lock multiplier (pure geometry, no fit).

10.4 Forward-time restriction and half-index classes

Distinguish an underlying integer class $\tau_V^{(\text{top})} \in \mathbb{Z}$ from the forward-time effective class:

$$\tau_V^{(\text{eff})} = \frac{1}{2}\, \tau_V^{(\text{top})}, \qquad \tau_V^{(\text{top})} \in \mathbb{Z}. \tag{60}$$

In particular, the effective class $\tau_V^{(\text{eff})} = 3/2$ corresponds to $\tau_V^{(\text{top})} = 3$.

10.5 Reciprocal radius scaling and the seam-lock multiplier

Let (R_e, r_e) denote the baseline (electron) toroidal projection and (R_V, r_V) the vector-channel $(u \leftrightarrow d)$ projection. Define the major-radius stretch factor

$$s_V := \frac{R_V}{R_e}. \tag{61}$$

Toroidal invariance (56) forces reciprocal contraction of the minor radius:

$$R_V r_V = R_e r_e = {\lambda_C}^2 \quad \Rightarrow \quad \frac{r_V}{r_e} = \frac{1}{s_V}. \tag{62}$$

The holonomy defect integral Δ_V samples the projected torsion density on the forward-time ribbon; in the seam picture, the net effect of stretching the path while thinning the tube is a multiplicative seam-lock correction that we take to be

$$\mathcal{S}_{\text{tor}} := s_V, \tag{63}$$

i.e. the observable defect is enhanced by the geometric path stretch enforced by (56).

10.6 Octant taxonomy gives a concrete number (no tuning)

In the $N = 8$ octant taxonomy, the minimal nontrivial forward-time odd class $\tau_V^{(\mathrm{top})} = 3$ activates a single unpaired octant generator per independent adjacency loop. The corresponding minimal pitch is one octant step $\Delta\theta_{\mathrm{oct}} = \pi/4$ per half-turn π, giving

$$\tan\beta_V = \frac{\Delta\theta_{\mathrm{oct}}}{\pi} = \frac{1}{4}, \qquad s_V = \sec\beta_V = \sqrt{1+\tan^2\beta_V} = \frac{\sqrt{17}}{4} \approx 1.0308. \tag{64}$$

Thus the required few-percent seam normalization in M6 is identified with a rigid geometric factor dictated by the octant model.

10.7 Minimal ansatz for $\mathcal{M}_V(\alpha)$

Adopt a minimal expansion

$$\mathcal{M}_V(\alpha) = 1 + \beta_{V,1}\,\alpha + \beta_{V,2}\,\alpha^2 + \beta_{V,3}\,\alpha^3 + \cdots, \tag{65}$$

with $\beta_{V,k}$ pure numbers fixed by the explicit weak packing map (not fitted).

10.8 Aether rotational ratio as the hierarchy footprint (optional lock)

Introduce the Aether rotational ratio

$$\rho_{e:a} := \frac{m_{\mathrm{e}}}{m_a}. \tag{66}$$

If the channel selection rules require an additional hierarchy suppression, retain the seam-lock ansatz

$$\Xi_{V,0} = \kappa_V\,\rho_{e:a}^{r}, \qquad \kappa_V \in \mathbb{Z}, \quad r \in \mathbb{N}, \tag{67}$$

with r fixed by geometry (not tuned). Combining (59), (63), and (67) yields the final seam normalization:

$$\Xi_V(\alpha) = \kappa_V\,\rho_{e:a}^{r}\,s_V\,\mathcal{M}_V(\alpha). \tag{68}$$

10.9 Consequences for $|V_{ud}|^2$

With antipodal bulk cancellation, $\varepsilon_V \approx \Delta_V$ and

$$|V_{ud}|^2 \propto \frac{1}{\mathcal{B}_{\mathrm{hol}}} = 1 - \Delta_V(\alpha)^2 + O(\Delta_V^3). \tag{69}$$

Using $\Delta_V = \frac{1}{8}\tau_V\,\Xi_V$,

$$\Delta_V(\alpha) = \frac{1}{8}\,\tau_V\,\kappa_V\,\rho_{e:a}^{r}\,s_V\,\mathcal{M}_V(\alpha), \tag{70}$$

and therefore

$$|V_{ud}|^2 = 1 - \frac{1}{64}\,\tau_V^2\,\kappa_V^2\,\rho_{e:a}^{2r}\,s_V^2\,\mathcal{M}_V(\alpha)^2 + O(\Delta_V^3). \tag{71}$$

10.10 M5 deliverable

Milestone M5 is complete once: (i) the toroidal projection radii (R, r) are explicitly mapped for the $u \leftrightarrow d$ packing, (ii) the octant pitch rule fixing s_V is derived from the seam graph selection rules (yielding (64)), (iii) $\mathcal{M}_V(\alpha)$ is derived from the explicit weak packing map (fixing $\beta_{V,k}$ in (65)), and (iv) if required, r and κ_V are fixed as discrete channel indices by the same selection rules.

11 Milestone M6: Numerical closure scan for a small-integer obstruction index

This milestone is diagnostic: it asks whether the observed row-1 deficit corresponds to a small (possibly half) integer obstruction class once the toroidal seam-lock multiplier s_V (Milestone M5) is included.

11.1 Measured closure residual

Define the first-row residual

$$\Delta_{\text{row1}} := (|V_{ud}|^2 + |V_{us}|^2 + |V_{ub}|^2) - 1. \tag{72}$$

Using (7), a representative central value is

$$\Delta_{\text{row1}} \approx -1.7 \times 10^{-3}. \tag{73}$$

11.2 Minimal quantized-seam model with toroidal seam-lock

In the small-defect regime (M7), $\Delta_{\text{row1}} = -(\Delta_{ud}^2 + \Delta_{us}^2 + \Delta_{ub}^2) + O(\Delta^3)$. For the diagnostic scan we use a single-index surrogate:

$$\Delta_{\text{row1}}^{(\text{APM})} = -\frac{1}{64}\,\tau_{\text{row1}}^2\,\mathcal{S}_p(\alpha)\,, \tag{74}$$

where τ_{row1} is an effective obstruction index and $\mathcal{S}_p(\alpha)$ is the dimensionless seam normalization.

Two low-order families are

$$\mathcal{S}_p^{(A)}(\alpha) = \alpha^p, \tag{75}$$

$$\mathcal{S}_p^{(B)}(\alpha) = (2\pi\alpha)^p. \tag{76}$$

To incorporate Milestone M5, multiply the normalization by the toroidal seam-lock multiplier $\mathcal{S}_{\text{tor}} = s_V$ from (63), with

$$s_V = \sec\beta_V = \frac{\sqrt{17}}{4} \approx 1.0308 \tag{77}$$

as derived by the minimal octant pitch rule in (64). Thus a torus-locked variant of the p-family is

$$\mathcal{S}_{p,\text{tor}}(\alpha) := s_V^2\,\mathcal{S}_p(\alpha). \tag{78}$$

Solving (74) gives

$$|\tau_{\mathrm{row1}}| = \frac{8\sqrt{|\Delta_{\mathrm{row1}}|}}{\sqrt{\mathcal{S}_p(\alpha)}}, \qquad |\tau_{\mathrm{row1}}|_{\mathrm{tor}} = \frac{8\sqrt{|\Delta_{\mathrm{row1}}|}}{\sqrt{s_V^2\,\mathcal{S}_p(\alpha)}} = \frac{|\tau_{\mathrm{row1}}|}{s_V}. \tag{79}$$

p	$\lvert\tau_{\mathrm{row1}}\rvert$ from α^p	$\lvert\tau_{\mathrm{row1}}\rvert$ from $(2\pi\alpha)^p$	$\lvert\tau_{\mathrm{row1}}\rvert_{\mathrm{tor}}$ from $s_V^2(2\pi\alpha)^p$
0	0.33	0.33	0.32
1	3.86	1.54	1.49
2	45.20	7.19	6.97
3	529.13	33.60	32.60
4	6.19×10^3	156.90	152.20
5	7.25×10^4	732.74	711.05
6	8.49×10^5	3.42×10^3	3.32×10^3

Table 1: Milestone M6 scan: inferred obstruction index magnitude $|\tau_{\mathrm{row1}}|$ required to reproduce $|\Delta_{\mathrm{row1}}| \approx 1.7\times10^{-3}$ under (74). The torus-locked column includes the geometric seam-lock multiplier s_V from Milestone M5.

11.3 Interpretation and uncertainty propagation

The only low-order case producing an $O(1)$ obstruction index is the $(2\pi\alpha)^p$ family at $p = 1$. With the toroidal seam-lock included, one obtains

$$|\tau_{\mathrm{row1}}|_{\mathrm{tor}} \approx 1.49, \tag{80}$$

which is numerically consistent with the half-integer class $3/2$ expected under forward-time restriction (M5).

Using (7) as a two-component uncertainty on the sum, the implied one-sigma band for the inferred $p = 1$ torus-locked index remains close to the half-integer hypothesis:

$$|\tau_{\mathrm{row1}}|_{\mathrm{tor}} \text{ in a representative range } \approx 1.13 \text{ to } 1.78. \tag{81}$$

11.4 Half-integer obstruction class and the 3/2 hypothesis

Write the half-class relation (as in M5)

$$\tau_{\mathrm{row1}}^{(\mathrm{eff})} = \frac{1}{2}\,\tau_{\mathrm{row1}}^{(\mathrm{top})}, \qquad \tau_{\mathrm{row1}}^{(\mathrm{top})} \in \mathbb{Z}, \tag{82}$$

so $\tau_{\mathrm{row1}}^{(\mathrm{top})} = 3$ corresponds to $|\tau_{\mathrm{row1}}^{(\mathrm{eff})}| = 3/2$.

A convenient measure of proximity to $3/2$ is

$$|\tau_{\mathrm{row1}}|_{\mathrm{tor}} \approx \frac{3}{2}\big(1 + \delta_{\mathrm{tor}}\big), \qquad \delta_{\mathrm{tor}} := \frac{|\tau_{\mathrm{row1}}|_{\mathrm{tor}}}{3/2} - 1 \approx -4 \times 10^{-3}, \tag{83}$$

i.e. a sub-percent residual once the toroidal seam-lock is applied.

11.5 Where the remaining mismatch belongs (it is $\mathcal{M}_V(\alpha)$)

To make explicit that the residual is not a topology change, rewrite the $p = 1$ torus-locked model as

$$\Delta_{\mathrm{row1}}^{(\mathrm{APM})} = -\frac{1}{64}\left(\tau_{\mathrm{row1}}^{(\mathrm{eff})}\right)^2 \left(s_V^2\, 2\pi\alpha\right) \mathcal{M}_V(\alpha)^2, \tag{84}$$

where s_V is fixed geometrically by (64) and $\mathcal{M}_V(\alpha)$ is the charge-basis-constrained basis-map multiplier introduced in (57) and expanded in (65).

Assuming the minimal half-class $\tau_{\mathrm{row1}}^{(\mathrm{eff})} = 3/2$, the value of $\mathcal{M}_V(\alpha)$ required to match the representative central residual (73) is

$$\mathcal{M}_V(\alpha) \approx 0.996, \tag{85}$$

i.e. a sub-percent basis-map correction of the size naturally expected from higher-order terms in (65), without introducing any new continuous normalization parameter.

11.6 Milestone M6 deliverable

Milestone M6 is complete once: (i) the toroidal seam-lock multiplier s_V is fixed by the explicit seam graph selection rule (M5), (ii) the $p = 1$ torus-locked family in (84) is adopted as the minimal closure surrogate, and (iii) $\mathcal{M}_V(\alpha)$ is derived from the packing map (fixing $\beta_{V,k}$ in (65)) so that the $3/2$ class becomes a prediction rather than an inference.

12 Milestone M7: Transfer and consistency across overlaps, channels, and observables

Milestone M7 requires that the same torsion/seam machinery transfers to the other first-row overlaps and remains consistent with prior holonomy bookkeeping elsewhere in the APM program.

12.1 Apply the obstruction formalism to V_{us} and V_{ub}

Define sector-specific forward-time defects Δ_{uq} for $q \in \{d, s, b\}$:

$$\Delta_{uq} := \frac{1}{2\pi h_e} \int_{\Sigma(\gamma_{uq,+})} (I - \Pi)\mathcal{T}_{uq}, \tag{86}$$

and impose the seam reduction

$$\Delta_{uq} = \frac{1}{8}\,\tau_{uq}\,\Xi_{uq}(\alpha), \qquad \tau_{uq} \in \mathbb{Z}. \tag{87}$$

A working physical expectation (to be formalized by explicit packing maps) is that strangeness-changing kaon-sector channels may occupy different adjacency neighborhoods or seam-energy sectors (heavier quark packing changes which seams are activated), allowing different κ_{uq}, r_{uq}, or admissible τ_{uq} classes while preserving the same structural mechanism.

12.2 Unified row-1 residual as a discrete-class prediction

In the small-defect regime,

$$\Delta_{\mathrm{row1}} = -\left(\Delta_{ud}^2 + \Delta_{us}^2 + \Delta_{ub}^2\right) + O(\Delta^3), \tag{88}$$

so

$$\Delta_{\mathrm{row1}} = -\frac{1}{64}\left(\tau_{ud}^2\,\Xi_{ud}(\alpha)^2 + \tau_{us}^2\,\Xi_{us}(\alpha)^2 + \tau_{ub}^2\,\Xi_{ub}(\alpha)^2\right) + O(\Delta^3). \tag{89}$$

12.3 Charge-basis conversion universality

Enforce

$$\Xi_{uq}(\alpha) = \kappa_{uq}\,\rho_{e:a}^{r_{uq}}\,\mathcal{M}_V(\alpha), \tag{90}$$

with the *same* $\mathcal{M}_V(\alpha)$ as in M5. Differences across sectors are permitted only through discrete indices κ_{uq} and discrete exponents r_{uq}, not through continuous refits of the α-dependent map.

12.4 M7 deliverable

Milestone M7 is complete once: (i) explicit torsion densities $\mathcal{T}_{us}$, $\mathcal{T}_{ub}$ are written for the relevant packings, (ii) (90) is enforced without introducing new continuous map parameters, and (iii) (89) yields small-integer classes across the first row (or falsifies the minimal octant-seam model).

13 First-row unitarity as packing-basis closure

With overlap definitions $V_{ud} = \langle u|d\rangle$, $V_{us} = \langle u|s\rangle$, $V_{ub} = \langle u|b\rangle$, (1) becomes

$$\sum_{q\in\{d,s,b\}} |\langle u|q\rangle_{\mathcal{H}}|^2 = 1, \tag{91}$$

a completeness statement of the down-type basis in the holonomy-induced inner product.

Using (7), the empirical target is $\Delta_{\mathrm{row1}} \approx -1.7 \times 10^{-3}$ as recorded in (73).

13.1 Where a deviation can originate in APM

Within the QMU ledger, a persistent $\Delta_{\mathrm{row1}} \neq 0$ arises via only two mechanisms:

(A) Holonomy leakage. Non-vanishing defect integrals produce incomplete closure in (91).

(B) Charge-basis conversion inconsistency. A charge-sector or normalization mismatch violates the unified charge equation bookkeeping; operationally, this manifests as an inconsistent SI↔QMU bridge (CCF usage) rather than a geometric holonomy defect.

14 Predictions and experiments (QMU phrasing)

P1 (closure-as-geometry). First-row unitarity is a holonomy-induced basis closure identity (91); deviations classify into (A) holonomy leakage vs (B) charge-basis conversion inconsistency.

P2 (constancy-as-closure). Superallowed $\mathcal{F}t$ constancy is (12): a universal $\mathcal{T}_V^{(*)}$ after boundary and charge-basis conversion terms are accounted in (13).

E1 (nuclear-structure vs holonomy discrimination). Because PDG emphasizes the role of nuclear-structure uncertainty in the superallowed V_{ud} budget Particle Data Group [2024], a QMU test is to separate $\mathcal{B}_{\text{hol}}$ and $\mathcal{B}_{\text{map}}$ explicitly: if the residual is dominated by nucleus-dependent modeling, it should localize in $\mathcal{B}_{\text{map}}$ rather than in a universal $\mathcal{B}_{\text{hol}}$.

E2 (channel redundancy). Independent V_{ud} channels (neutron and pion beta) provide orthogonal constraints on whether the same universal $\mathcal{B}_{\text{hol}}$ applies across distinct packing environments Particle Data Group [2024].

15 Roadmap summary to a parameter-free derivation

This paper implements Milestones M1–M7 as Sections 6–12. A parameter-free completion requires the explicit weak packing action (M1–M2), the explicit seam graph and selection rules (M3–M4), the derived charge-basis-constrained basis-map multiplier and seam-lock selection (M5), and then transfer and cross-channel consistency (M7) with the diagnostic scan (M6) providing a concrete target class.

A Bridge to standard $\mathcal{F}t$ reporting

Experimental superallowed analyses report $\mathcal{F}t$ in seconds and quote correction factors as percent-level multipliers. This appendix provides only a translation layer into QMU.

The dimensionless QMU invariant is $\mathcal{T}_V = F_q \mathcal{F}t$ from (11). To translate numerical values, map F_q into s^{-1} using the QMU conversion tables Thomson [2025b], then form $\mathcal{T}_V$. All correction factors entering $\mathcal{B}_V$ remain dimensionless and transfer unchanged.

B Constants reference (CODATA)

For SI-anchored constants used in bridging calculations, we use the most recent CODATA recommended values available in the open literature at the time of writing, namely the 2022 adjustment report Mohr et al. [2025].

Acknowledgments

The Quantum AetherDynamics Institute (QADI) is a private 501(c)(3) research institute developing the Aether Physics Model (APM) and Quantum Measurement Units (QMU) Thomson III

[2025]. Publications and data are archived with DOIs in the AetherPhysics Zenodo community: zenodo.org/communities/aetherphysics.

References

Nicola Cabibbo. Unitary symmetry and leptonic decays. *Physical Review Letters*, 10:531–533, 1963. doi: 10.1103/PhysRevLett.10.531. URL https://doi.org/10.1103/PhysRevLett.10.531.

Andrzej Czarnecki, William J. Marciano, and Alberto Sirlin. Radiative corrections to neutron and nuclear beta decays revisited. *Physical Review D*, 100:073008, 2019. doi: 10.1103/PhysRevD.100.073008. URL https://doi.org/10.1103/PhysRevD.100.073008.

J. C. Hardy and I. S. Towner. Superallowed $0^+ \to 0^+$ nuclear β decays: 2020 critical survey, with implications for v_{ud} and ckm unitarity. *Physical Review C*, 102:045501, 2020. doi: 10.1103/PhysRevC.102.045501. URL https://doi.org/10.1103/PhysRevC.102.045501.

Makoto Kobayashi and Toshihide Maskawa. Cp-violation in the renormalizable theory of weak interaction. *Progress of Theoretical Physics*, 49:652–657, 1973. doi: 10.1143/PTP.49.652. URL https://doi.org/10.1143/PTP.49.652.

William J. Marciano and Alberto Sirlin. Radiative corrections to beta decay and the possibility of a fourth generation. *Physical Review Letters*, 56:22–25, 1986. doi: 10.1103/PhysRevLett.56.22. URL https://doi.org/10.1103/PhysRevLett.56.22.

Peter J. Mohr, David B. Newell, Barry N. Taylor, and Eite Tiesinga. Codata recommended values of the fundamental physical constants: 2022. *Journal of Physical and Chemical Reference Data*, 54(3):033105, September 2025. doi: 10.1063/5.0279860. URL https://physics.nist.gov/cuu/Constants/. Published online 16 September 2025.

Particle Data Group. v_{ud}, v_{us}, the cabibbo angle, and ckm unitarity. *Progress of Theoretical and Experimental Physics*, 2024(8):083C01, 2024. doi: 10.1093/ptep/ptae084. URL https://pdg.lbl.gov/2024/reviews/rpp2024-rev-vud-vus.pdf. PDG Review of Particle Physics online review PDF.

Chien-Yes Seng, Mikhail Gorchtein, and Michael J. Ramsey-Musolf. Dispersive evaluation of the inner radiative correction in semileptonic beta decay. *Physical Review D*, 100:013001, 2019. doi: 10.1103/PhysRevD.100.013001. URL https://doi.org/10.1103/PhysRevD.100.013001.

David Thomson. The charge conversion factor in the aether physics model: From singular to distributed charge, with rules, exceptions, and benchmarks, October 2025a. URL https://doi.org/10.5281/zenodo.17451188.

David Thomson. Reference tables for quantum measurement unit (qmu) conversions: Cgs and mks systems, November 2025b. URL https://doi.org/10.5281/zenodo.17683574.

David W. Thomson III. Quantum aetherdynamics institute (qadi): Community doi overview and citation guide. Zenodo, 2025. URL https://doi.org/10.5281/zenodo.17479314.

Lincoln Wolfenstein. Parametrization of the kobayashi-maskawa matrix. *Physical Review Letters*, 51:1945–1947, 1983. doi: 10.1103/PhysRevLett.51.1945. URL https://doi.org/10.1103/PhysRevLett.51.1945.